

Shear and extensional flows as drivers for the crystallisation of isotactic polypropylene

When rheology, microscopy and thermal analysis must meet

S. Filipe · B. Knogler · K. Buchmann · M. Obadal

Rheological Analysis of Polymers/Special Chapter
© Akadémiai Kiadó, Budapest, Hungary 2009

Abstract The article addresses the relevance of shear and uniaxial extensional flow behaviour on the crystallisation of isotactic polypropylenes differing in terms of molar mass distribution (MMD). The importance of combining several experimental techniques, namely rheological, thermal and microscopic, to follow the response of the material arising from the application of given processing conditions, is here demonstrated. Systems with a broader MMD possessing even residual amounts of high molar mass (M_M) tails were shown to be more prone to develop β -phase crystallites. The latter effect was seen to be a consequence of the application of a step shear at a temperature for which the formation of β -phase is known to be preferential.

Keywords Polypropylene · Flow-induced crystallisation · Uniaxial extensional flow · Orientation-induced nuclei

Introduction

Isotactic polypropylene (PP) is a highly versatile polymeric material covering a wide range of applications. Such variety of applications requires a well-defined molecular design of the polymer, which can be done by an

appropriate selection of the catalyst, co-catalyst, monomers and polymerisation conditions. This procedure allows the production of materials possessing a variety of physical properties. The modification of PP properties during compounding can be done alternatively by making use of its variability in terms of supermolecular structure; it is well-known that PP is a polymorphic material showing four crystalline modifications, namely monoclinic α -phase, trigonal β -phase, orthorhombic γ -phase and mesomorphic smectic phase [1–5]. Such features open several opportunities to nucleate a desired polymorph by the appropriate selection of a specific nucleating agent. For example, the use of sorbitol-based nucleators gives rise to materials with an excellent transparency and a rather good stiffness. The previous example has in fact, a high industrial relevance [6]. PP containing a predominant amount of β -phase is another example; in past years close interrelations between the β -form content and a significant increase of toughness and cold drawability have been reported [6–10] and even industrially utilised [11]. It is worth noting that PP possesses extremely high sensitivity to any factor during its crystallisation, which is favourable in respect to post-reactor modification. On the other hand, the high sensitivity of PP can cause some specific features during its processing, arising from the morphological gradients being created by the effect of processing conditions.

Molecular structural properties, such as M_M , MMD and branching are known to affect significantly both linear and non-linear viscoelastic properties [12, 13]. Such knowledge is particularly relevant for polypropylenes, especially when considering their high sensitivity towards flow-induced crystallisation (either under shear, elongation or mixed types of flow, accompanying always polymer processing) [14–17]. Moreover, it is undeniable that extensional flows and non-linear viscoelasticity have a relevant role during

S. Filipe (✉) · B. Knogler · M. Obadal
Borealis Polyolefine GmbH, InnoTech Operational Support,
Advanced Polymer Characterisation, Sankt Peter Strasse 25,
4021 Linz, Austria
e-mail: susana.filipe@borealisgroup.com

K. Buchmann
Borealis Polyolefine GmbH, InnoTech Operational Support,
Analytical and Physical Testing Laboratory, Sankt Peter Strasse
25, 4021 Linz, Austria

processes such as film extrusion and melt blown. That justifies the need of a more deep insight on the relationship between molecular structural properties, extensional flow behaviour and its effects on flow-induced crystallisation. Knowledge on the relevant molecular and rheological aspects affecting flow-induced crystallisation under shear was gathered along the last years [14–17]. The mechanisms and different flow regimes governing flow-induced crystallisation were shown to depend on the reptation and stretching times of the overall molar mass distribution (MMD). The presence of high molar mass tails revealed to be crucial on the enhancement of the crystallisation kinetics. The stretching and final orientation of these chains was shown to be a function of the Deborah number and total applied shear strain [18].

The shear and extensional flow properties, as well as the crystallisation structure under shear for materials differing in terms of high M_M tails content, will be here addressed. Overall, the combination of several factors exerting at individual structural levels can complicate the scenario on the comparison of the polymer behaviour during a crystallisation experiment or throughout processing; in other words, the behaviour under quiescent and shear conditions can differ significantly. One of such examples is described in this work showing a need to combine several experimental techniques to understand specific phenomena during polymer solidification.

Experimental

Materials

Two commercially available isotactic polypropylenes (PP1 and PP2) with very similar characteristics were used in this study. Both materials are characterised by a melt-flow index (MFI) of $2.5 \text{ g } 10 \text{ min}^{-1}$ (503.15 K, 2.16 kg, ISO 1133), an average molar mass (M_M) of approximately $520,000 \text{ g mol}^{-1}$ and an isotacticity index of 0.982 (infrared spectroscopy, Chicco index). The materials contained a standard stabilisation based on phenol–phosphite stabilisers, namely Irganox 1010 produced by Ciba Specialty Chemicals Inc., and calcium stearate (used as an acid scavenger).

Methods

Molecular characterisation

High temperature gel permeation chromatography (GPC) was performed in order to characterise the materials with respect to their average molar mass (M_M) and MMD. All the GPC measurements were performed at 413.15 K using trichlorobenzene (TCB) as solvent.

Rheological characterisation

The materials were characterised in terms of their rheological properties under both small amplitude oscillatory shear (SAOS) and uniaxial extensional flow.

SAOS measurements were carried out on a stress controlled rotational rheometer Anton Paar MCR 501 using a parallel plate geometry of 25 mm and a gap of 1.3 mm. The SAOS experiments were performed under nitrogen atmosphere, applying temperatures ranging from 473.15 to 533.15 K, and setting a strain within the linear viscoelastic regime.

The relaxation spectrum was determined using the master curves of G' , G'' data determined for a reference temperature of 473.15 K. The software used for the calculation of the relaxation spectrum was IRIS 2006. The relaxation spectrum was used to determine the relaxation spectrum index and the longest reptation time, following the same procedure described elsewhere [14, 19].

Particularly, care was taken for the preparation of the samples for extensional flow. The samples were prepared by compression moulding at 503.15 K followed by slowly cooling to room temperature (forced water or air cooling were not used). This procedure allowed obtaining well-shaped samples free of residual stresses.

The uniaxial extensional flow measurements were conducted on an Anton Paar MCR 501 coupled with the Sentmanat extensional fixture (SER). The temperature for the uniaxial extensional flow measurements was set at 453.15 K, applying extension rates ranging from 0.01 to 10 s^{-1} .

Flow-induced crystallisation

Isothermal crystallisation experiments were carried out under both quiescent and shear conditions using a strain controlled rotational rheometer ARES (Rheometric Scientific). The kinetics of crystallisation with and without application of shear was studied at 405.15 K using a cone-plate geometry (cone angle = 1°). The flow-induced crystallisation kinetics was done as follows: first, the samples were subjected to annealing at 513.15 K, for 15 min, in order to erase any thermal history, stresses and/or residual crystalline structures, arising from sample preparation. The annealing procedure was followed by cooling from 513.15 to 413.15 K at $10 \text{ }^\circ\text{C min}^{-1}$ and from 413.15 K to the crystallisation temperature, 405.15 K, applying a cooling rate of $2 \text{ }^\circ\text{C min}^{-1}$. The protocol used for the cooling process was applied in order to minimise problems related with a high temperature gradient coming from the mass of the tool, oven, etc.

For the quasi-quiescent, a steady shear experiment was used applying continuously a very low shear rate of 0.01 s^{-1} . The crystallisation kinetics was monitored through the

evolution of the shear viscosity with time. The isothermal experiments under shear were done by applying a step shear of 0.25 s^{-1} for 200 s, followed by monitoring of the shear viscosity. Several types of experiments were done, in order to evaluate the effect of total applied strain, time of application of step shear and applied shear, on the kinetics of crystallisation. These results will however not be shown here.

The discs prepared during these experiments were rapidly quenched and used for further observation under light microscopy.

Nucleation density measurement

The measurement of nucleation density was performed at Johannes Kepler University in Linz, Austria, using an in-house developed counter current method. Basically, a cylindrical sample with approximately 4-mm diameter and 20-mm length is quenched to the desired crystallisation temperature. In order to achieve a high initial cooling rate the sample is initially rinsed from one end with a fast moving fluid of a temperature below the target crystallisation temperature. When a thermocouple embedded along the centre-line of the sample (recording the temperature–time profile) detects a passing of the target temperature, a counter current of a fluid of the desired crystallisation temperature is applied. This results in a rapid achievement of T_c . The number of spherulites per unit of volume N_c is then calculated using the approximation $N_c = N_A^{3/2}$, where N_A is a number of spherulites per area counted from polarised-light micrographs made on cross-sections of the cylindrical specimens. More details about the method can be found elsewhere [20, 21].

Isothermal crystallisation

A DSC Q2000 differential scanning calorimeter, TA Instruments was used. Nitrogen was used as a purge gas constantly passing (50 mL s^{-1}) through the heat sink and over the cell. Discs with diameter of 4 mm and thickness of 200- μm thick were loaded (approximately 4 mg) into standard aluminium sample pans and heated to 483.15 K, then held at this temperature for 5 min to erase previous thermal history and subsequently rapidly cooled to a given T_c (403.15, 405.15 and 407.15 K). The end of the crystallisation was indicated by the end of the exothermic crystallisation peak. After an integration of the exothermic peak, the half time of crystallisation $t_{0.5}$ was taken as a point at which the crystallisation is 50% completed.

Spherulitic morphology

The spherulitic morphology of the specimens prepared by the use of rotational rheometry was observed with the

aid of polarised-light microscopy (PLM). Thin slices ($\sim 20 \mu\text{m}$) were microtomed approximately 2 mm from the edge of the circular specimen perpendicularly to its diameter. Micrographs of the slices were taken using an Olympus BX50 microscope connected with an A4I imaging system.

Results and discussion

Differential scanning calorimetry and nucleation density

After the processing of PP1 and PP2, namely cast film production and subsequent biaxial orientation, the PP2 film showed special inhomogeneities on the final film surface as compared to the PP1. It is worth to note that the final morphology and macroscopic appearance of drawn films basically arises as a legacy of the original morphology in the initial cast films [22, 23]. One of the important factors, among others, influencing the morphology formation is the material crystallisability. A common and fast way to screen it is a non- or isothermal experiment being performed using differential scanning calorimetry. One should be aware in this matter of the effect of several parameters, namely a real relation between instrument and sample temperature, a contact area between the pan and sample or cooling rate; it is thus highly recommended to use virtually not only a similar mass, but also a similar shape for the samples—a disc cut out from thin plate serves perfectly. In this work, an isothermal experiment was chosen and performed at 403.15, 405.15 and 407.15 K. Crystallisation is detected by an exothermic peak on a heat flow–time curve; the decrease of the crystallisation temperature causes sharpening and narrowing of the exothermic peak; its integration according to a time implies an increase of relative crystallinity as a function of crystallisation time. Then, the crystallisation half time $t_{0.5}$, defined as the time spent from the onset of crystallisation to the point, where the crystallisation is 50% complete, can be easily obtained. In Fig. 1 the crystallisation half time $t_{0.5}$ for PP1 and PP2 is plotted as a function of crystallisation temperature T_c . Generally, $t_{0.5}$ exponentially increases with increasing T_c . In this case it is evident that the $t_{0.5}$ values are substantially higher for PP2, which indicates its slower crystallisation process as compared to PP1.

Both parts of the crystallisation process should be considered when explaining such behaviour—these are the nucleation and the growth. As reported [24], the growth rate of iPP is particularly driven by the stereoregularity of the polymer chain which is not, however, relevant for the case of PP1 and PP2 as both possess virtually identical isotacticity. Then, it is needed to consider the nucleation stage, i.e. the number of active nuclei. Actually, from

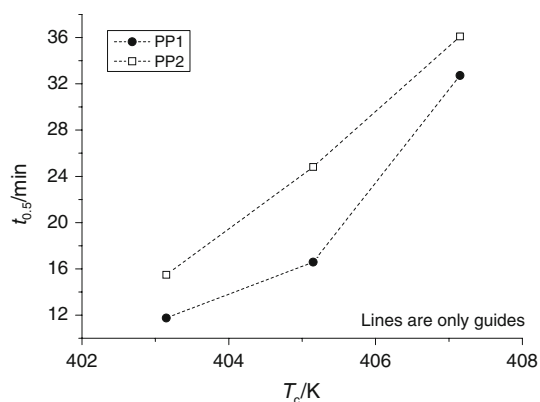


Fig. 1 Half time of crystallisation $t_{0.5}$ as a function of crystallisation temperature T_c . Lines are guides to the eyes

initial microscopy investigations it seemed that PP2 showed the lower nucleation density (i.e. lower number of spherulites), which can be further quantified by several methods [see more details, e.g. in Ref. 25]; at this work a counter current method was used, see [20, 21]. In Fig. 2, the number of nuclei versus crystallisation temperature is showed; it is apparent that the PP1 indicates an order of magnitude higher nucleation density as compared to PP2. Assuming the material homogeneity and the fact that both materials are not nucleated, the phenomenon can be related to the presence of any other heterogeneous particles like catalyst residua, non-specified solid particle contamination or variation in MMD. However, the latter effect does not fit to the fact that the broader MMD of PP2 should lead to a higher number of nuclei, as generally accepted in the literature [24, 25].

The difference in nucleation density obviously influence the overall crystallisation process, however, it should be emphasized that the experiments were done so far at quiescent conditions. In order to get then an overall picture, the solidification behaviour should be screened also at variable dynamic conditions and the rheological properties

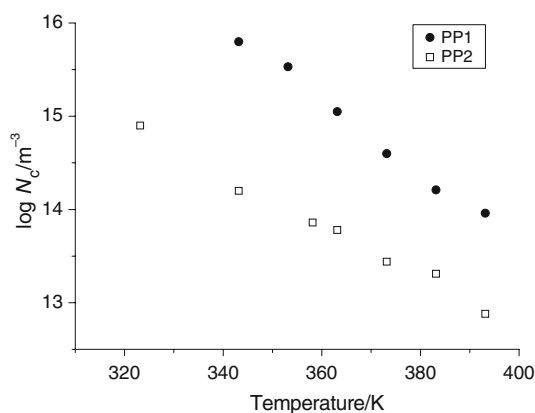


Fig. 2 Nucleation density N_c as a function of temperature

under shear and extension should be as well, carefully screened.

Rheological analysis

It is well recognized that the application of both shear and extensional flows, encountered during polymer processing, are remarkably affecting the crystallisation kinetics. The mechanism driving flow-induced crystallisation is highly sensitive to small differences in terms of molecular structural properties (e.g. M_M and MMD). The dominance of extensional flows, typical of processes such as film extrusion, blow moulding, etc., has to be taken into account when considering flow-induced crystallisation. Previous research showed that extensional flows are much more effective than shear flows, in what regards flow-induced crystallisation [26–28]. This is mainly due to the higher level of molecular orientation, achieved as a result of extensional flow. A good understanding of the relationship between molecular structural properties (e.g., M_M , MMD and topology) and the rheological flow behaviour under shear and extensional flow is thus required.

Small amplitude oscillatory shear (SAOS)

When looking solely at the rheological flow curves from SAOS one can say that the materials do not show pronounced differences (Fig. 3). However, a more in deep analysis of the results, namely the relaxation spectrum, proved that the materials are actually possessing different thermal rheological complexities (Fig. 4). First point worth of remark is that the flow activation energies of both materials slightly deviate from the typical values known for linear high isotactic PPs, 40 kJ mol^{-1} [29, 30] (Table 1). The flow activation energies (45.50 and 46.04 kJ/mol for PP1 and PP2, respectively) are, however, below the values typically seen for branched i-PP (ranging usually from 50

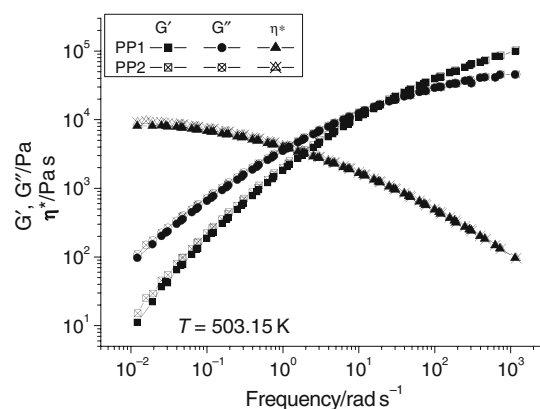


Fig. 3 Small amplitude oscillatory shear data at 503.15 K

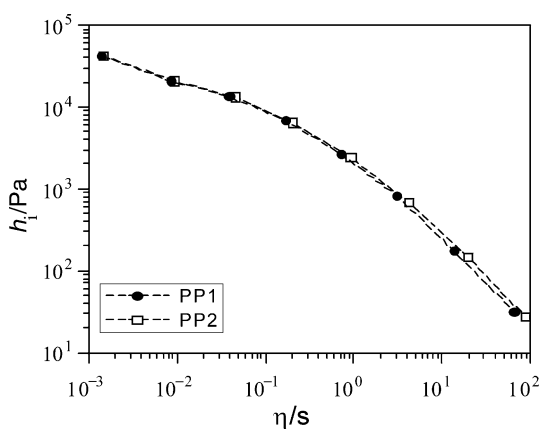


Fig. 4 Continuous relaxation time spectra determined from small amplitude oscillatory shear data

to 60 kJ mol⁻¹) [29, 30]. Therefore, one can argue that the additional thermal rheological complexity of the materials arises not from long-chain branching (LCB), but rather from the presence of a residual amount of high molar mass tails and a stronger level of entanglements. When considering only the flow activation energy one might consider that PP1 and PP2 are behaving similarly in what regards shear flow. However, a shift of the characteristic relaxation time λ_c towards higher values together with an increase of the relaxation spectrum index seen for PP2, show that the material has in fact a higher thermal rheological complexity, higher elasticity and broader relaxation mechanisms (Table 1). Such observation is consistent with a broader MMD, as determined using GPC (Table 1).

The analysis of the relaxation spectrum allowed capturing different relaxation mechanisms arising from polydispersity. An important parameter that can be estimated from the relaxation spectrum is the longest reptation time, λ_{rep_long} . This parameter represents a measure of the relaxation of the high molar mass tails present in the material [13]. The higher values of the longest reptation time seen for PP2 in comparison to PP1 (89.3 against 66.3 s) are an evidence that the number of high molar mass tails in PP2 is higher.

Uniaxial extensional flow

Regarding the rheological behaviour under uniaxial extensional flow, one can state that there is an overall shift

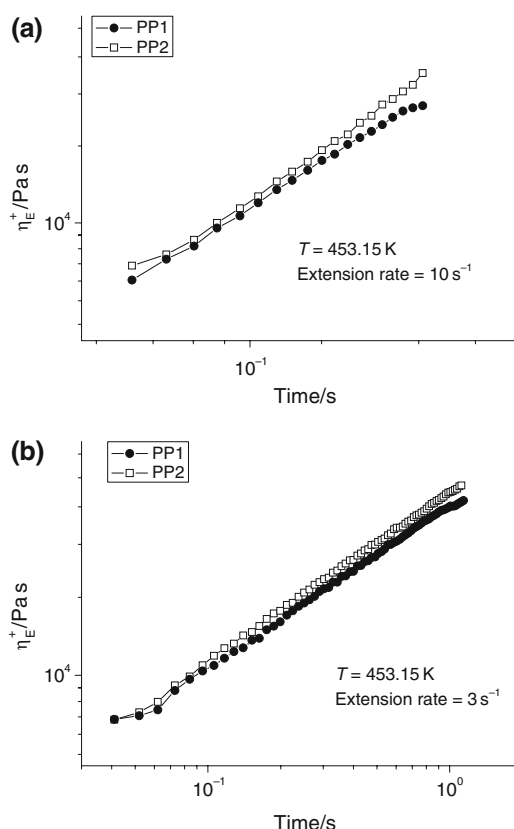


Fig. 5 Uniaxial extensional flow behaviour at 453.15 K. **a** Extension rate of 10 s⁻¹ and **b** extension rate of 3 s⁻¹

of the elongational viscosity towards higher values for PP2 (Fig. 5). Second, for the highest extensional rate (10 s⁻¹) one can observe that, above a critical Hencky strain of about 2.19, the increase of the uniaxial extensional viscosity seen for PP2 is higher than the one observed for PP1 (Fig. 5). Moreover, it can be stated that above this Hencky strain the uniaxial extensional viscosity of PP1 coincides with the linear viscoelastic envelop (LVE), whereas for PP2, a clear deviation towards higher values is observed. Such behaviour is usually defined as strain hardening and can arise either from the presence of high molar mass tails or from the presence of LCB [31, 32]. Since the system does not possess LCB, one can assume that the residual strain hardening here observed arises in this case, from the presence of high molar mass tails. Even if residual, such molecular chains with higher M_M might lead to a higher

Table 1 GPC and rheological parameters determined from small amplitude oscillatory shear at 473.15 K

Materials	M_M	MMD	Characteristic relaxation time λ_c/s	PDI	Flow activation energy $E_a/kJ mol^{-1}$	Relaxation spectrum index (RSI)	Longest reptation time λ_{rep_long}/s
PP1	514.9	7.5	0.096	6.11	45.50	45.5	66.3
PP2	518.0	8.5	0.100	6.06	46.04	50.4	89.3

PDI an MWD calculated from SAOS and GPC, respectively

resistance to disentanglement, while the material is being stretched under uniaxial extensional flow. A similar effect was observed by Münstedt [31] and Takahashi et al. [32]. The evidence of strain hardening behaviour observed for PP2 is consistent with the findings under SAOS. According with SAOS, the time needed for the relaxation of the high molar mass tails ($\lambda_{\text{rep_long}}$) was shown to be higher for PP2 than for PP1 (Table 1).

The different rheological nature of PP1 and PP2 previously discussed has naturally to be encountered when considering flow-induced crystallisation.

Flow-induced crystallisation

Previous research proved that MMD and M_M have a strong influence on the mobility and orientation of the molecular chains under flow, thus affecting at a latter stage, the crystallisation process [33]. Both mobility and orientation of the molecular chains during flow (either shear or extensional flow) are driven by the entanglement density (related with zero shear viscosity, plateau modulus), the elasticity of the system (G' , Relaxation Spectrum) and the interactions between the different molecular chains (Relaxation Spectrum). As already shown, PP1 and PP2 differ in terms of their rheological behaviour under both shear and extension (Table 1, Figs. 3, 4, 5). Due to their different nature in terms of long-relaxation mechanisms, it is expected that the application of similar conditions of total deformation (under either shear or extension) will lead to a different response in terms of the kinetics of crystallisation.

The flow-induced crystallisation measurements done under shear conditions (applying a step shear of 0.25 s^{-1} for 200 s) showed that the crystallisation kinetics of PP2 starts

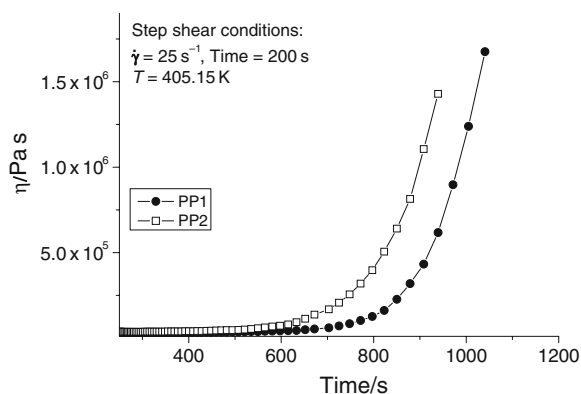


Fig. 6 Rheological behaviour for flow-induced crystallisation test applying a step shear of 0.25 s^{-1} for 200 s at 405.15 K. The experimental procedure included annealing at 513.15 K for 15 min, followed by cooling until 405.15 K at $10^\circ/\text{min}$ and finally application of a step shear. The figure depicts only the evolution of shear viscosity with time after application of the step shear

earlier than the one of PP1 (Fig. 6). This is quite surprising, since these results are contradicting the nucleation density measurements and the isothermal crystallisation, for which PP1 was showing a higher nucleation and a faster crystallisation, as compared to PP2 (Figs. 1, 2). Such discrepancy might be explained by the fact that the isothermal crystallisation, as well as the nucleation density measurements, were done under quiescent conditions. The application of shear is known to have an impact on the crystallisation kinetics, as well as on the formation of α - and β -phases [34]. Moreover, when considering the crystallisation induced by flow, it is clear that under isothermal conditions a system possessing high molar mass tails (higher polydispersity) is more likely to give rise to oriented structures. That seems to be the case of PP2. If present, due to their longer relaxation mechanisms, longer chains previously subjected to a prior orientation during the flow process are more prone to keep their orientation. After cessation of the flow, these oriented structures can then act as some sort of ‘orientation-induced nuclei’, which can lead to a further increase of the relaxation times of the high molar mass chains and enhance even more the flow-induced crystallisation process. This can explain the faster crystallisation under shear flow observed for PP2. In order to confirm this hypothesis, the discs used for the flow-induced crystallisation measurements were analysed using light microscopy.

Light microscopy

Considering that PP1 and PP2 material possess different rheological behaviour, particularly in uniaxial extension, one could imagine that such phenomena would significantly influence the morphology development during crystallisation under shear or elongation. Figure 7 shows morphologies of the specimens prepared from discs crystallised in the rheometer. While PP1 possesses strictly spherulitic morphology (i.e. virtually isotropic) the PP2 shows a morphology with several elongated aggregates, see also detail in Fig. 8. Such morphology is a typical consequence of the shear-induced crystallisation of iPP when substantial amount of the row nuclei are created, as a

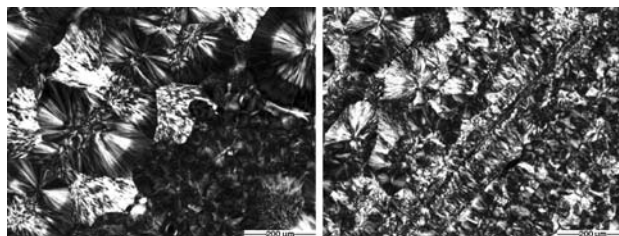


Fig. 7 Morphology of specimen prepared applying a step shear of 0.25 s^{-1} for 200 s using a temperature of 405.15 K; *left*—PP1, *right*—PP2

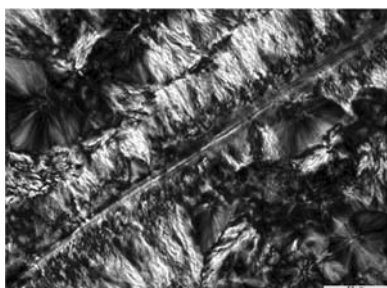


Fig. 8 Detail of the shear-induced morphologies in PP1 prepared applying a step shear of 0.25 s^{-1} for 200 s using a temperature of 405.15 K

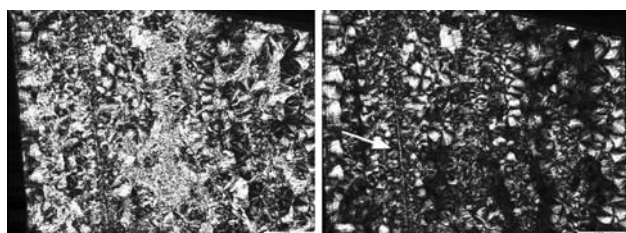


Fig. 9 Partial melting of the β -phase overgrowths in PP2; *left*—room temperature, *right*—428.15 K. Some of the β -phase overgrowth is marked by a *white arrow* in the right micrograph

consequence of the higher concentration of longer chains. Basically, the row nuclei, being created first, consist of α -phase; however, these α -row nuclei can via point-like β -nuclei present on their surfaces nucleate the β -phase if its growth rate is higher than the growth rate of α -phase. In such case, the cylindrical growth of α -phase is terminated by the β -phase spherulitic growth; the phenomenon is well described in Ref. [35]. The assignment of the overgrowths to β -phase can be observed from partly melted material showed in Fig. 9. At a temperature of 428.15 K the β -phase structures are separately melted and only α -phase morphologies remain.

Conclusions

It is now relevant to point out that the intensive row-nuclei formation driven by the presence of longer polymer chains must be also considered as a main factor explaining the discrepancy between the crystallisation behaviour of PP1 and PP2 under quiescent and shear conditions. Due to their longer relaxation times, high molar mass tails subjected to a prior orientation (either under shear and/or elongation) are prone to keep their orientation once flow is ceased. Such phenomena leads to the formation of oriented α structures (raw nuclei), which can under appropriate

conditions nucleate and lead to the formation of both α - and β -phases. The present work shows that a good combination of several experimental techniques, namely rheological, thermo-analytical and microscopic, is essential to elucidate such phenomena during polymer solidification.

Acknowledgements The authors would like to thank E. Utenthaler for the SAOS measurements, Christian Samhaber for the isothermal crystallisation measurements and to J. Wolfschwenger for the GPC data. Prof. G. Eder and Dr. E. Ratajski are greatly acknowledged for the nucleation density measurements. An acknowledgement is due to Dr. J. Reussner for his continuous support.

References

1. Padden FJ, Keith HD. Spherulitic crystallisation in polypropylene. *J Appl Phys.* 1959;30:479–85.
2. Natta G, Corradini P. Structure and properties of isotactic polypropylene. *Nuovo Cimento Suppl.* 1960;15:40–51.
3. Turner-Jones A, Aizlewood JM, Beckett DR. Crystalline forms of isotactic polypropylene. *Makromol Chem.* 1964;75:134–58.
4. Varga J. β -Modification of isotactic polypropylene: preparation, structure, processing, properties, and application. *Macromol Sci Phys.* 2002;41:1121–71.
5. Varga J. Crystallization melting and supermolecular structure of isotactic polypropylene. In: Karger-Kocsis J, editor. *Polypropylene: structure, blends and composites*, vol. 1. London: Chapman & Hall; 1995.
6. Kristiansen PM, Gress A, Smith P, Nanft D, Schmidt HW. Phase behavior, nucleation and optical properties of the binary system isotactic polypropylene/*N, N', N''*-tris-isopentyl-1, 3, 5-benzene-tricarboxamide. *Polymer.* 2006;47:249–53.
7. Tjong SC, Shen JS, Li RKY. Morphological behaviour and instrumented dart impact properties of β -crystalline-phase polypropylene. *Polymer.* 1996;37:2309–16.
8. Karger-Kocsis J. How does phase transformation toughening work in semicrystalline polymers? *Polym Eng Sci.* 1996;36:203–10.
9. Kotek J, Raab M, Baldrian J, Grellmann W. The effect of specific β -nucleation on morphology and mechanical behavior of isotactic polypropylene. *J Appl Polym Sci.* 2002;85:1174–84.
10. Obadal M, Čermák R, Baran N, Stoklasa K, Šimoník J. Impact strength of β -nucleated polypropylene. *Int Polym Process.* 2004;19:35–9.
11. http://www.borealisgroup.com/pdf/literature/borealis-borouge/product-news/K_PN_No_29_GB_PF_2007_10_BB.pdf.
12. Gotsis AD, Zeevenhoven BLF. Effect of long branches on the rheology of polypropylene. *J Rheol.* 2004;48:895–914.
13. Sugimoto M, Masubuchi Y, Takimoto J, Koyama K. Melt rheology of polypropylene containing small amounts of high-molecular-weight chain. 2. Uniaxial and biaxial extensional flow. *Macromolecules.* 2001;34:6056–63.
14. Meerveld J, Peters GWM, Hütter M. Towards a rheological classification of flow induced crystallization experiments of polymer melts. *Rheol Acta.* 2004;44:119–34.
15. Balzano L, Rastogi S, Peters GWM. Flow induced crystallization in isotactic polypropylene-1, 3:2, 4-bis(3, 4-dimethylbenzylidene)sorbitol blends: implications on morphology of shear and phase separation. *Macromolecules.* 2008;41:399–408.
16. Nogales A, Hsiao BS, Somani RH, Srivinas S, Tsou AH, Balta-Calleja FJ, et al. Shear-induced crystallization of isotactic polypropylene with different molecular weight distributions: in situ

- small- and wide-angle X-ray scattering studies. *Polymer*. 2001;42:5247–56.
17. Baert J, Van Puyvelde P. Effect of molecular and processing parameters on the flow-induced crystallization of poly-1-butene. Part I: kinetics and morphology. *Polymer*. 2006;47:5871–9.
 18. Baert J, Van Puyvelde P, Langouche F. Flow-induced crystallization of PB-1: from the low shear rate region up to processing rates. *Macromolecules*. 2006;39:9215–22.
 19. U.S. Patent 5,998,558.
 20. Janeschitz-Kriegl H, Ratajski E, Wippel H. The physics of a thermal nuclei in *polymer* crystallization. *Colloid Polym Sci*. 1999;277:217–26.
 21. Stadlbauer M, Eder G, Janeschitz-Kriegl H. Crystallization kinetics of two aliphatic polyketones. *Polymer*. 2001;42:3809–16.
 22. Olley RH, Basset DC. On surface morphology and drawing of polypropylene films. *J Macromol Sci Phys*. 1994;33:209–27.
 23. Hobbs SY, Pratt CF. The development of surface texture in blown polypropylene film. *Polym Eng Sci*. 1982;22:594–600.
 24. Gahleitner M, Bachner C, Ratajski E, Rohaczek G, Neißl W. Effects of the catalyst system on the crystallization of polypropylene. *J Appl Polym Sci*. 1999;73:2507–15.
 25. Gahleitner M, Bernreitner K, Neißl W. Crystallisation and mechanical properties of polypropylene homopolymers as influenced by molecular structure and nucleation. *Polym Test*. 1995;14:173–87.
 26. Stadlbauer M, Janeschitz-Kriegl H, Lipp M, Eder G, Ratajski E. New extensional rheometer for creep flow at high tensile stress. Part II. Flow induced nucleation for the crystallization of iPP. *J Rheol*. 2004;48:631–40.
 27. Stadlbauer M, Janeschitz-Kriegl H, Lipp M, Eder G, Forstner R. Extensional rheometer for creep flow at high tensile stress. Part I. Description and validation. *J Rheol*. 2004;48:611–30.
 28. Hadinata C, Boos D, Gabriel C, Wassner E, Rüllmann M, Kao N, et al. Elongation-induced crystallization of a high molecular weight isotactic polybutene-1 melt compared to shear-induced crystallization. *J Rheol*. 2007;51:195–216.
 29. Yamaguchi M, Wagner MH. Impact of processing history on rheological properties for branched polypropylene. *Polymer*. 2006;47:3629–35.
 30. Eckstein A, Suhm J, Friedrich C, Maier RD, Sassmannshausen J, Bochmann M, et al. Determination of plateau moduli and entanglement molecular weights of isotactic, syndiotactic, and atactic polypropylenes synthesized with metallocene catalysts. *Macromolecules*. 1998;31:1335–40.
 31. Muenstedt H. Dependence of the elongational behavior of polystyrene melts on molecular weight and molecular weight distribution. *J Rheol*. 1980;24:847–68.
 32. Takahashi T, Takimoto JH, Koyama K. Elongational viscosity for miscible and immiscible polymer blends. II. Blends with a small amount of UHMW polymer. *J Appl Polym Sci*. 1999;72:961–9.
 33. Vleeshouwers S, Meijer HEH. A rheological study of shear induced crystallization. *Rheol Acta*. 1996;35:391–9.
 34. Somani R, Hsiao BS, Nogales A, Fruitwala H, Srivinas S, Tsou AH. Structure development during shear flow induced crystallization of i-PP: in situ wide-angle X-ray diffraction study. *Macromolecules*. 2001;34:5902–9.
 35. Varga J, Karger-Kocsis J. Rules of supermolecular structure formation in sheared isotactic polypropylene melts. *J Polym Sci B Polym Phys*. 1996;34:657–70.